

1
2
3
4
5
6
7
8
9
10
11
12
13
14
15
16
17
18
19
20
21
22
23
24
25

Interpreting coronary artery disease GWAS results: A functional genomics approach assessing biological significance

Katherine Hartmann^{1*#a}, Michał Seweryn², Wolfgang Sadee¹

¹ Department of Cancer Biology and Genetics, Center for Pharmacogenomics, College of Medicine, The Ohio State University, Columbus, OH, USA

² Biobank Lab, Department of Molecular Biophysics, University of Lodz, Poland

^{#a} Current Address: Department of Internal Medicine, Santa Clara Valley Medical Center, San Jose, CA, USA

* Corresponding Author

E-mail: hartmann.kate@gmail.com (KH)

26 **Abstract**

27 Genome-wide association studies (GWAS) have implicated 58 loci in coronary artery
28 disease (CAD). However, the biological basis for these associations, the relevant genes, and
29 causative variants often remain uncertain. Since the vast majority of GWAS loci reside outside
30 coding regions, most exert regulatory functions. Here we explore the complexity of each of
31 these loci, using tissue specific RNA sequencing data from GTEx to identify genes that exhibit
32 altered expression patterns in the context of GWAS-significant loci, expanding the list of
33 candidate genes from the 75 currently annotated by GWAS to 245, with almost half of these
34 transcripts being non-coding. Tissue specific allelic expression imbalance data, also from GTEx,
35 allows us to uncover GWAS variants that mark functional variation in a locus, e.g., rs7528419
36 residing in the *SORT1* locus, in liver specifically, and rs72689147 in the *GUYC1A1* locus,
37 across a variety of tissues. We consider the GWAS variant rs1412444 in the LIPA locus in
38 more detail as an example, probing tissue and transcript specific effects of genetic variation in
39 the region. By evaluating linkage disequilibrium (LD) between tissue specific eQTLs, we reveal
40 evidence for multiple functional variants within loci. We identify 3 variants (rs1412444,
41 rs1051338, rs2250781) that when considered together, each improve the ability to account for
42 LIPA gene expression, suggesting multiple interacting factors. These results refine the
43 assignment of 58 GWAS loci to likely causative variants in a handful of cases and for the
44 remainder help to re-prioritize associated genes and RNA isoforms, suggesting that ncRNAs
45 maybe a relevant transcript in almost half of CAD GWAS results. Our findings support a multi-
46 factorial system where a single variant can influence multiple genes and each genes is
47 regulated by multiple variants.

48

49 **Introduction**

50 Genome-wide association studies (GWAS) have identified dozens of genetic variants
51 (SNPs) associated with cardiovascular disease risk and related clinical phenotypes (*e.g.*, blood
52 pressure, lipid levels) (1–3). However, these findings do not necessarily translate to
53 understanding of heritability, likely because we do not fully understand the link between
54 significant loci, causative genetic variants and complex phenotypes (4). Moreover, the
55 functional variant and even the relevant gene close to a significant locus in many cases remain
56 uncertain. The majority of statistically significant SNPs reside in non-coding regions with poorly
57 defined biological functions and a complex architecture of multiple genes and transcripts (5).
58 Gene assignment is largely based on proximity, usually with little consideration for non-coding
59 transcripts in the locus or the possibility of chromatin looping that places distant regions in close
60 proximity (6), with regulatory domains often interacting with multiple genomic target regions (9).
61 Additionally, localization to non-coding regions means the mechanisms remain unknown as the
62 function is not immediately obvious, while implicating epigenetics and other regulatory
63 processes (5,7). This uncertainty limits the utility of GWAS findings. To interpret and refine
64 GWAS results for coronary artery disease (CAD), we use RNA expression, in addition to
65 physical position, to prioritize the variants and gene(s) most likely to be relevant.

66 Although largely thought of in a single SNP – single protein-coding gene paradigm,
67 GWAS variants mark regions with various degrees of complexity often including several protein-
68 coding and non-coding RNAs (ncRNAs). SNPs located within RNA exons may not only alter the
69 protein sequence but also influence RNA structure and function in a transcript specific manner
70 (8). Some of these GWAS loci consist of gene clusters that are coordinately regulated (9), and
71 almost all include multiple RNA isoforms expressed from a given gene, including splice
72 isoforms. Within such multi-gene regions, a single variant may affect more than one gene, both
73 protein-coding and non-coding, via chromatin looping between multiple sites or by regulating
74 DNA accessibility for the entire region (9,10). Therefore, a critical question for interpreting

75 GWAS associations is which gene(s), and what specific transcript(s), are affected within each
76 significant locus.

77 The potential for multiple variants to affect a single gene is also critical to the
78 interpretation of GWAS. Such interactions between variants, either linear or dynamic (epistasis)
79 and dictated by linkage disequilibrium (LD), may remain hidden in GWAS because of the
80 restrictive nature of multiple hypotheses corrections; however targeted analysis of loci reveals
81 multiple interacting variants modulating gene expression (9,11,12). Failure to identify all main
82 functional variants in a gene locus and their interactions results in false estimates of the genetic
83 influence of a locus, and further impedes discovery of dynamic interactions that are sensitive to
84 partial or confounded estimates (13–18).

85 Detailed analysis of RNA expression to evaluate GWAS results is increasingly employed
86 to evaluate co-localization of GWAS and eQTL signals (19–21). However, most methods rely
87 on the a *priori* assumptions that variants are independent of each other (e.g., eCAVIAR), while
88 COLOC assumes that there is only one functional variant per GWAS locus. These assumptions
89 do not allow for a multifactorial system, where a single variant can influence multiple genes and
90 each gene can be regulated by multiple variants. Accordingly, we search for overlap between
91 variants marking GWAS associations and those marking eQTLs rather than using existing
92 methods to co-localize signals. Although this approach limits our power to detect overlap as it
93 requires a single variant appear as a marker in both GWAS and eQTL analysis, we posit it
94 facilitates functional exploration of a multi-factorial system.

95 A recent CAD GWAS used 1000 genomes to impute insertions/deletions, rare variants
96 and common variants that were not directly genotyped as part of a large-scale meta-analysis of
97 185 thousand cases and controls (1). While confirming 47 of the 48 previously identified loci,
98 this study identified an additional 10 at genome-wide significance, bringing the total count of
99 CAD associated loci to 58. Each of these loci are based on robust statistical associations for
100 one or more SNPs in the locus. Furthermore, each locus has been assigned one or more

101 genes based largely on proximity as part of the GWAS annotation. We consider each of these
102 58 loci in detail, using QTL and position to re-prioritize candidate genes and focusing on a
103 subset of loci, to begin resolving inherent complexities of genomic architecture.

104

105 **Materials and Methods**

106 **Data**

107 **1000 Genomes**

108 Genotypes for calculating LD between SNPs of interest were downloaded from:
109 http://ftp.1000genomes.ebi.ac.uk/vol1/ftp/release/20130502/supporting/GRCh38_positions/.
110 Individuals of the 'EUR' superpopulation were selected for LD calculations.

111 **CATHeritization GENetics (CATHGEN)**

112 Expression, genotypes, and clinical phenotypes were acquired via dbGaP Project #5358
113 (dbGaP accession phs0000703). Expression levels had been determined using Illumina
114 HumanHT-12-v3 in RNA from whole blood. We considered variables recorded in pht003672:
115 age (phv00197199), gender (phv00197207), hypercholesterolemia (phv00197204), smoking
116 (phv00197208), number of diseased vessels (phv00197295), and history of myocardial
117 infarction (MI) (phv00197212). We restricted analysis to Caucasians (race (phv00197206)) for
118 sample size considerations (862 Caucasians; 259 African Americans). The approach developed
119 here can be extended to other ethnic groups as these datasets become available. Data access
120 was approved by the Ohio State University IRB (Protocol #2013H0096).

121 **Genotype and Tissue Expression Project (GTEx)**

122 Tissue-specific RNAseq data was acquired via dbGaP Project #5358 (dbGaP accession
123 phs000424). For details see Lonsdale et al. and
124 <http://www.gtexportal.org/home/documentationPage> (22). MI was defined as recorded history of

125 heart disease (MHHRTDIS) or heart attack (MHHRTATT). Data access was approved by the
126 Ohio State University IRB (Protocol #2013H0096).

127 **Gene Information**

128 Transcripts, coding status, GO Ids, number of publications indexed in PubMed,
129 gene/transcript expression, GWAS hits, GTEx eQTLs (expression quantitative trait loci) and
130 sQTLs (splicing quantitative trait loci) including tissue specific expression, and allelic ratios in
131 DNase hypersensitivity sites were obtained for each gene using the package 'mgIR'
132 implemented in R (<https://cran.r-project.org/web/packages/mgIR/index.html>). Protein-coding
133 transcripts were defined as those annotated by BiomaRt as "IGC gene", "IGD gene", "IG gene",
134 "IGJ gene", "IGLV gene", "IGM gene", "IGV gene", "IGZ gene", "nonsense_mediated_decay",
135 "nontranslating CDS", "non stop decay", "polymorphic pseudogene", "TRC gene", "TRD gene",
136 "TRJ gene", "protein_coding", "TEC". The remaining designations were considered non-coding
137 and include "disrupted domain", "IGC pseudogene", "IGJ pseudogene", "IG pseudogene", "IGV
138 pseudogene", "processed_pseudogene", "transcribed_processed_pseudogene", "transcribed
139 unitary pseudogene", "transcribed_unprocessed_pseudogene", "translated processed
140 pseudogene", "TRJ pseudogene", "unprocessed_pseudogene", "unitary_pseudogene", "3prime
141 overlapping ncna", "ambiguous orf", "antisense", "antisense RNA", "lincRNA", "ncna host",
142 "processed_transcript", "sense intronic", "sense overlapping", "lincRNA", "retained_intron",
143 "miRNA", "miRNA_pseudogene", "miscRNA", "miscRNA_pseudogene", "Mt rRNA", "Mt tRNA",
144 "rRNA", "scRNA", "snlRNA", "snoRNA", "snRNA", "tRNA", "tRNA_pseudogene", and
145 "rRNA_pseudogene". A gene was considered non-coding only if all transcripts were non-coding.

146 **Linkage Disequilibrium (LD)**

147 R^2 was calculated for 1000 genomes 'EUR' super population using the 'ld' function from
148 the package 'snpStats' implemented in R and using LDlink.

149 **Association Testing**

150 Additive logistic models to account for LIPA expression and MI using different
151 combinations of variants were compared using ANOVA with a likelihood ratio test (LRT)
152 implemented in R. Gender and age were included as covariates in models explaining LIPA gene
153 expression, while sex, age, hypercholesterolemia, smoking, and number of diseased vessels
154 were included as covariates in models explaining MI. Differences in LIPA expression between
155 those with or without a history of MI were calculated using the `wilcoxin.test` function in R.
156 Bonferroni multiple hypothesis correction was implemented.

157 **Allelic Expression Imbalance (AEI)**

158 Allelic RNA expression imbalance (AEI) was assessed using data from GTEx
159 (`phe000039.v1.GTEx_v8_ASE.expression-matrixfmt-ase.c1`). Candidate variants were
160 subsetted from each individual file, and the deviation of the “REF_RATIO” from the
161 “NULL_RATIO” was plotted for each variant in a given tissue type. Tissue types with 5 or more
162 samples were considered.

163

164 **Results and discussion**

165 **Expanding candidate gene lists using QTL and position**

166 As many functional variants marked by GWAS likely have regulatory functions affecting
167 RNA expression or processing, the same SNPs appearing in GWAS may also mark expression
168 Quantitative Trait Loci (eQTLs) or splicing Quantitative Trait Loci (sQTLs) for their target gene.
169 To assign GWAS hits to target genes, we determine for each of the GWAS SNPs whether it
170 appears as an eQTL or sQTL reported by GTEx, searching all available tissues. Recognizing
171 that often multiple SNPs exist over a genomic region as significant GWAS hits, we consider
172 each one individually in assigning candidate genes and separately assess concordance. We opt

173 not to use COLOC and other existing tools that search for overlapping signal between GWAS
174 variants and QTLs because they make assumptions about the genetic model that are not in line
175 with the multi-factorial system we test here (23); namely, these methods assume a single
176 causative variant or that each variant acts independently. Instead, although we recognize it
177 limits the overlap we are able to detect and biases our sample to variants that are ideal markers
178 (i.e. frequent), we search for exact matches between GWAS and QTL marker variants. In
179 addition to evaluating associations with gene expression and splicing, we consider the physical
180 position of each GWAS variant as SNPs within the RNA sequence are expected to impact RNA
181 folding, stability, function, etc. Specifically, we consider the corresponding gene for any
182 transcript that physically overlaps the GWAS variant regardless of strand, thus incorporating
183 coding, non-coding, and antisense genes. Using these three approaches (cis-eQTLs, cis-
184 sQTLs, position), we expand the list of potential candidate genes for the 58 GWAS loci from 75
185 to 245 (Fig 1A, S1 File, comprehensive table is included in S3 File, S1 Fig).

186

187 **Fig 1. Summary of CAD GWAS loci.** (A) For each of the 58 loci identified by GWAS,
188 number of candidate genes annotated by GWAS and additional genes added by eQTL, then
189 sQTL, and finally position based reprioritization, if implicating genes other than those annotated
190 previously by GWAS (See S1 Fig for further details about the approach and S3 File for a
191 comprehensive table). Tier 1 (n = 7) denotes those loci where a GWAS annotated gene is
192 supported by QTL-based re-prioritization or position and no other candidate genes are
193 introduced; Tier 2 (n = 50) where QTL-based reprioritization or position introduces new
194 associated genes while supporting all candidates at this locus (Tier2A), only some including the
195 GWAS gene (Tier2B) or new genes except the GWAS genes (Tier2C); and Tier 3 (n = 1) where
196 no eQTLs or sQTLs are identified and no gene physically overlaps the SNP, accordingly
197 annotation by GWAS is not supported and no other genes are implicated. (B) For each of the
198 245 candidate genes displayed along the x-axis (names available in S1 File), the number of

199 transcripts assigned to the gene, the number of antisense transcripts (note: antisense genes are
200 not included among the 245 candidate genes unless their expression is associated with or they
201 physically overlap a GWAS variant), GO terms, Papers indexed in PubMed, *cis*-eQTLs and
202 sQTLs published in v8 of GTEx. Blue bar highlights those genes with only non-coding
203 transcripts.

204

205 In an effort to identify those loci where a target gene(s) is clearly supported by functional
206 markers, we consider the agreement between the gene assignment given by GWAS studies
207 and that derived by eQTL and sQTL analysis as well as by physical position. We group each of
208 the 58 GWAS loci as follows: GWAS annotation is supported by QTL-based re-prioritization or
209 position and no other candidate genes are introduced (Tier 1); QTL-based reprioritization or
210 position introduces new genes, while supporting all (Tier2A), some (Tier2B), or none (Tier2C) of
211 the genes annotated by GWAS so that multiple genes are implicated; no eQTLs or sQTLs are
212 identified and no gene or annotated RNA transcript physically overlaps the SNP, accordingly
213 annotation by GWAS is not supported (but also not negated) and no other genes are implicated
214 (Tier 3), see Fig 1, S2 Fig, S3 File.

215 In some instances, the number of candidate genes implicated changes substantially with
216 the particular GWAS SNP considered (S3 File). Nikpay et al. report both the SNP originally
217 identified in CAD GWAS studies and the most promising SNP in the same locus they identified
218 in a large-scale meta-analysis using 1000 genomes imputation to incorporate variants with
219 lower minor allele frequency (1). We consider both in our analysis, and for 11 of 32 loci with
220 multiple SNPs find the tier classification changes depending on the SNP considered (S3 File).
221 For example, locus 10 - rs2252641 and rs17678683 (ZEB2, AC074093.1), rs2252641, which
222 was implicated in historic GWAS studies, is annotated as ZEB2 and AC074093.1, but based on
223 QTL and position is not associated with any gene and would be considered as Tier3 while
224 rs17678683, identified by Nikpay et al. is an eQTL in skeletal muscle for ZEB2 and an sQTL in

225 subcutaneous adipose also for ZEB2 and would thus be considered as Tier1. The two SNPs
226 have an $R^2 < 0.2$.

227 This discordance between variants in the same locus may represent a weakness of our
228 approach that looks for overlap with an individual SNP rather than considering ‘colocalization’
229 more broadly. However, it occurs almost exclusively among SNPs that are in relatively poor LD
230 (frequently $R^2 < 0.2$) and would not be expected to serve as good markers for one another nor
231 be part of the same haplotype. Alternatively, this discordance may represent multiple functional
232 variants in the locus with different target genes. Regardless, our results emphasize the
233 complexity in elucidating functional variants from GWAS results.

234

235 **Tier 1: No new candidate genes introduced – GWAS annotation supported**

236 For 7 loci, QTL-based reprioritization and/or position supports the GWAS annotation
237 without introducing new candidate genes, supporting all or some of the gene(s) annotated by
238 GWAS: locus 16 - rs6903956 (ADTRP), locus 32 - rs11203042 and rs1412444 (LIPA), locus 38
239 - rs9319428 (FLT1), locus 42 - rs17514846 (FURIN, FES), locus 54 - rs7212798 (BCAS3),
240 locus 57 - rs11830157 (KSR2), and locus 8 - rs6544713 (ABCG8; however ABCG5 also
241 annotated by GWAS is not supported by QTL or position) (Table 1).

242

243 **Table 1. Tier 1 CAD GWAS loci**

Locus	SNP	OR	Risk Allele (Freq)	Gene	eQTL Tissue(s)	sQTL Tissue(s)	Position
16	rs6903956	1.65 ^a (1.44-1.90)	A (0.08 ^a)	ADTRP		Testis	ADTRP (intron)

32	rs11203042	1.04 (1.02-1.06)	T (0.45)	LIPA	Adipose (subq) Adipose (visceral) Colon (transverse) Heart (atrium) Lung Pancreas Skin (sun exp) Spleen Thyroid Blood	Adipose (subq) Fibroblasts Lung	LIPA (intron)
32	rs1412444	1.07 (1.05-1.09)	T (0.37)	LIPA	Adipose (subq) Adipose (visceral) Adrenal Gland Artery (aorta) Brain (cerebellum) Colon (sigmoid) Colon (transverse) Heart (atrium) Heart (LV) Lung Skeletal Muscle Nerve Pancreas Skin (not sun exp) Skin (sun exposed) Spleen Stomach Thyroid Blood	Adipose (subq) Adipose (visceral) Adrenal Gland Artery (aorta) Artery (tibial) Brain (spinal cord) Breast Fibroblasts Lymphocytes Lung Tibial Nerve Pancreas Skin (sun exposed) Small Intestine Spleen Stomach Blood	LIPA (intron)
38	rs9319428	1.04 (1.02-1.06)	A (0.31)	FLT1	Nerve (tibial)		FLT1 (intron)
42	rs17514846	1.05 (1.03-1.07)	A (0.44)	FES	Adipose (subq) Adipose (visceral) Adrenal Gland Artery (aorta) Artery (tibial) Fibroblast Colon (transverse) Esophagus (musc.) Heart (atrium) Lung Nerve (tibial) Pancreas Pituitary Prostate Skin (not sun exp) Skin (sun exposed) Stomach Thyroid Blood	Adipose (subq) Adipose (visceral) Artery (aorta) Artery (tibial) Breast Fibroblasts Colon (sigmoid) Esophagus (GEJ) Esophagus (musc.) Heart (atrium) Heart (LV) Lung Salivary Gland Nerve (tibial) Prostate Skin (not sun exp) Skin (sun exposed) Small Intestine Spleen Thyroid Blood	FURIN (intron)
				FURIN	Artery (aorta) Artery (tibial) Esophagus		
54	rs7212798			BCAS3			BCAS3 (intron)
57	rs11830157			KSR2			KSR2

08 ^b	rs6544713	1.05 (1.03-1.07)	T (0.32)	ABCG8	Colon (transverse)	(intron) ABCG8 (intron)
-----------------	-----------	---------------------	-------------	-------	--------------------	-------------------------------

244

245 Tissue names in grey font indicate GWAS SNP is associated with a decrease in gene
246 expression (eQTL) or normalized intron-excision ratio (sQTL), while those in black font are
247 associated with increased expression/normalized intron-excision ratio.

248

249 ^a values reported from original publication (24) in Han Chinese population. rs6903956 was not
250 significant in Nikpay et al. (1).

251 ^b ABCG8 and ABCG5 were both annotated by GWAS. ABCG5 was not supported by QTL or
252 position

253

254

For four of the loci (16-ADTRP, 32-LIPA, 38-FLT1, 42-FURIN, 8-ABCG8), GWAS

255 annotation of candidate gene assignment is supported by both QTL and position. In one

256 instance, locus 42 - rs17514846 (FURIN, FES), more than one gene is annotated by GWAS and

257 supported by our reprioritization. rs17514846, which falls in an intron of FURIN, serves as an

258 eQTL and an sQTL for FES in 23 tissues and an eQTL for FURIN in 3 tissues, two of which

259 (aorta and tibial artery) overlap with FES. In aorta and tibial artery, rs17514846 is associated

260 with decreased expression of FES as opposed to increased expression of FURIN – a possible

261 example of competing interactions between regulatory and promoter regions. Evidence for

262 multiple candidate genes in a locus may represent a paradigm in which a single SNP exerts an

263 impact through more than one gene.

264 In some instances the same variant in the same tissue is associated with both

265 expression and splicing. For example, rs141244 in blood is associated with increased

266 expression of LIPA and decreased splicing, a scenario that is consistent with greater stability of

267 the un-spliced transcript. Thus, in considering potential mechanisms of action for the variant, it

268 is important to evaluate not only the implications of increased levels of LIPA mRNA, but also

269 increased levels of the un-spliced transcript.

270

271 **Tier 2: New candidate genes implicated**

272 Variants in 50 loci are associated with expression of one or more genes or physically
273 overlap with another gene in addition to all (39 loci), some (7 loci), or none (4 loci) of the genes
274 annotated by GWAS. Loci where additional candidate genes are introduced are classified as
275 Tier 2 (S3 File). Candidate genes for these 50 GWAS loci are expanded by an average of 4.3
276 genes per locus for a total of 170 genes: 116 from eQTL based reprioritization, 17 from sQTL
277 based reprioritization, 5 from physical position, and 32 from some combination of these features
278 (S3 Fig).

279 While about a third of the loci (21) have two or fewer candidate genes, others have
280 substantially more: e.g., locus 33 - rs12413409 and rs11191416 (CYP17A1-CNNM2-NT5C2)
281 are associated with expression of twelve genes: ARL3, AS3MT, ATP5MD, BORCS7, CALHM2,
282 CNNM2, CYP17A1-AS1, MARCKSL1P1, MFSD13A, NT5C2, SFXN2, and WBP1L. Importantly,
283 these multi-gene eQTLs cannot be explained solely by co-expression between genes. These
284 eQTLs are often associated with expression of different genes in different tissues and for those
285 associations in the same tissue the genes are not necessarily co-expressed (25). Possible
286 mechanisms accounting for these relationships include a co-regulated gene cluster with master
287 regulator regions affecting all genes in that region (26,27). While we cannot exclude trans-acting
288 effects, these are typically smaller in size; allelic expression imbalance can serve to distinguish
289 between *cis* and *trans* effects, but robust RNA allelic ratios are often not available in GTEx.

290 Notably, ncRNAs are candidate genes for 33 of the 58 loci expanded from 6 loci prior to
291 re-prioritization. For no loci are all candidate genes non-coding. The greatest percent of non-
292 coding candidate genes (80%) is observed for locus 20 - rs12190287 and rs12202017 (TCF21).
293 The protein-coding gene TCF21 annotated by GWAS is supported by eQTLs in 24 different
294 tissues while 4 additional non-coding genes are introduced based on eQTL and sQTL analysis.
295 The candidate ncRNAs are located within a 500KB region, with TARID being antisense to
296 TCF21, and like many non-coding genes generally have lower expression levels.

297 For Tier 2C loci, there is no evidence to support the GWAS annotation. For example,
298 locus 46 - rs1122608 and rs56289821 LDLR is annotated by GWAS, a gene well-recognized for
299 its role in lipid metabolism; yet, rs1122608 falls within an intron of SMARCA4 and is both an
300 eQTL and sQTL for SMARCA4 as well as an eQTL for CARM1 and YIPF2 but not LDLR. The
301 alternative SNP identified by GWAS, rs56289821, also does not point to LDLR but rather
302 implicates RGL3, SLC44A2, and again SMARCA4. These 4 Tier 2C loci critically require future
303 work, both mechanistic and computational, to explore relevant gene targets.

304

305 **Tier 3: No genes implicated**

306 The remaining GWAS locus, locus 55 - rs663129 (MC4R, PMAIP1), classified as Tier 3,
307 did not show any association with expression of nearby genes and is not physically overlapping
308 any transcripts (S3 File). This locus and 3 others (locus 27 - rs2954029 (TRIB1), locus 54 -
309 rs7212798 (BCAS3), and locus 57 - rs11830157 (KSR2)) that are without any eQTL
310 associations may have more subtle or context-dependent effects on gene expression that
311 remain undetectable in GTEx. In particular, non-polyadenylated transcripts are not in GTEx as
312 poly-dT priming was used, leaving countless ncRNAs as additional candidates. Furthermore,
313 these SNPs may affect gene expression in *trans* (although we do not find such evidence in the
314 GTEx *trans*-eQTL dataset) or exert their effect without altering RNA levels measured by
315 RNAseq (e.g. by controlling the chromatin structure or co-translationally alter RNA
316 modifications). Additionally, variants affecting RNA functions and processing (structural RNA
317 SNPs) (8,28), may not be visible as eQTLs, or they may selectively affect translation by
318 changing polysomal loading (29).

319 Given GWAS variants are expected to mark functional variants rather than themselves
320 being functional, we test SNPs within a 1MB window in LD ($R^2 > 0.8$) with each of the 4 GWAS
321 variants lacking annotations, expanding the number of SNPs to 200. Using this approach, we

322 find significant eQTLs, but no significant sQTLs, for three of the four loci. For locus 57, we were
323 unable to find additional candidate SNPs with an $R^2 > 0.8$ to mark the haplotype.

324 For locus 55, without any candidate genes identified by our original re-prioritization,
325 eighteen variants (mean R^2 0.95 with the GWAS variant rs663129) are eQTLs in testis for
326 MC4R, also annotated by GWAS. Seven of these variants have an R^2 of 1 with the GWAS
327 variant. Five of these 18 SNPs fall within a non-coding RNA (AC090771.2) approximately 200kb
328 downstream of MC4R.

329 For locus 27, two variants (rs10808546 and rs2954031 with R^2 of 0.87 and 0.91 with the
330 GWAS variant rs2954029) are eQTLs in lung for a non-coding RNA (AC100858.3) almost 400kb
331 downstream and on the opposite strand to TRIB1. These two SNPs and 15 others in high LD
332 with the GWAS variant fall within an intron of a different non-coding RNA (AC091114.1), located
333 immediately upstream of TRIB1.

334 For locus 54, we find 83 variants (mean R^2 0.96 with the GWAS variant rs7212798) are
335 eQTLs in tibial artery and nerve for genes BCAS3, AC005884.1, and RP11-136H19.1. Five of
336 these variants with an R^2 of 1 with the GWAS variant serve as eQTLs for AC005884.1 in tibial
337 nerve, and are physically located within BCAS3, the protein-coding gene that has been
338 annotated by GWAS. A different five variants are eQTLs for BCAS3; they are identified in tibial
339 artery and have a mean R^2 with the GWAS variant of 0.81. Such long-range high LD values
340 imply evolutionarily conserved LD blocks with biological selectable functions.

341 Thus, by expanding the candidate SNP list to include other variants in strong LD with
342 that identified by GWAS over long genomic distances, we find additional candidate genes
343 supported by eQTL and physical position.

344

345 **Survey of CAD GWAS loci**

346 The genomic loci for each these 245 candidate genes often harbor multiple protein-
347 coding and non-coding transcripts arranged on both the sense and antisense strands (S2 File).
348 They express an average of 9 transcripts per gene and a maximum of 189 (TEX41- locus 10 -
349 rs2252641, rs17678683), with 47% of all transcripts being non-coding (Fig 1B). More than half
350 of the gene loci (161) also contain one or more antisense genes (i.e., located on the opposite
351 strand and overlapping).

352 Using GTEx data, we find RNA expression is associated with one or more genetic
353 variant in the locus with a median of 4 eQTLs (max 32230) among 50% of the 245 candidate
354 genes in 48 different tissues (Fig 1B).

355 With a median of 26 publications and a maximum of 27,497 (APOE), only a handful of
356 these 245 candidate genes have been well studied to date (Fig 1B). Twenty percent (51) of
357 genes do not have a single paper indexed in PubMed. There are on average 20 gene ontology
358 (GO) terms, which are manually curated based on the literature, assigned to each gene;
359 however, 62 (25%) of the candidate genes have no associated GO terms. We find those genes
360 without GO terms and with limited publications do not have fewer markers of functionality
361 (eQTLs, splicing QTLs, etc.), but are almost exclusively non-coding, indicative of a recognized
362 bias in the literature toward protein-coding genes (Fig 1).

363 Each implicated locus displays an astoundingly complex architecture with multiple
364 candidate genes implicated by RNA expression and physical location, each with a number of
365 overlapping coding and non-coding transcripts including those in antisense orientation. The
366 complexity of these loci emphasizes the need for targeted molecular studies and computational
367 approaches to determine the relevant gene and transcript(s). The distribution of PubMed
368 articles and GO ids across candidate genes suggests that this targeted work has touched on
369 only a handful of genes thus far, with more recent studies beginning to focus on 'neglected'
370 CAD candidate genes (30).

371

372 **Allelic RNA expression imbalance reveals functional** 373 **variation**

374 To evaluate potential functionality for each of the 58 GWAS loci, we ask whether each
375 candidate SNP is associated with allelic expression imbalance (AEI), a specific indicator of *cis*-
376 acting regulatory variation. Whereas comparing expression of the two alleles at a heterozygous
377 variant, various external/*trans*-acting influences on gene expression are shared and the *cis*-
378 acting effect of the heterozygous variant can be isolated. In the absence of a functional variant
379 altering RNA expression, the anticipated distribution between the alleles is 0.5 (ratio=1)(8,31).

380 Using data released by GTEx, we evaluate AEI at each of 104 candidate variants across
381 54 tissue types. Only 55 of the SNPs are represented in the data. The remainder likely are in
382 intergenic regions and poorly captured by RNA sequencing, while obtaining accurate AEI ratios
383 requires rather robust expression (>30 RPM)(32). Of the 55, many are present in only a few
384 samples making it difficult to infer differential expression. However, several SNPs show
385 surprisingly robust data – thousands of samples and counts for each allele in the dozens-
386 hundreds. A majority of these SNPs fail to reveal allelic expression imbalance, with near normal
387 distribution of deviation from the expected ratio, suggesting no correlation between the GWAS
388 variant and allelic expression imbalance. This implies that the GWAS candidate SNPs
389 represented in the data are actually relatively poor markers for functional *cis*-acting variants in
390 the locus; however, splicing events generating RNA isoforms with similar turnover are one
391 example where allelic expression imbalance would fail.

392 A number of SNPs do display consistent allelic expression imbalance (Fig 2). Locus 3 –
393 rs7528419 (SORT1), which falls in the 3'UTR of CELSR2 exhibits AEI in 53/57 liver samples.
394 Overall low expression of CELSR2 in liver tissue, however means that these ratios are for the
395 most part based on low coverage (median total count 13). Despite the relative consistency from
396 sample to sample, large allelic ratios derived from relatively low counts, as observed here,

397 raises suspicion for systemic sources of bias, e.g. preferential amplification of one allele. To
398 evaluate this further, we considered allelic ratios at nearby SNPs in strong LD ($R^2 > 0.9$) and
399 weak LD ($R^2 < 0.1$). As these SNPs are co-located, systemic sources of bias should affect all
400 SNPs in the locus while 'true' biological AEI would be expected only for those variants in strong
401 LD with a functional SNP. We observe AEI for those SNPs in strong LD with the GWAS marker,
402 but not for those in the same region in weak LD, a pattern that is suggestive of 'true' biological
403 AEI and a functional cis-acting variant.

404

405 **Fig 2. Allelic expression imbalance at GWAS variants mark functional SNPs.**

406 Deviation in the observed from the expected ratio for individuals heterozygous for given GWAS
407 variant. (A) Locus 3 – rs7528419 (SORT1) exhibits AEI in 53/57 liver samples. Subcutaneous
408 adipose, also shown, demonstrates near normal distribution of deviation from the expected
409 allelic ratio and is representative of the 46 other tissues with at least 5 samples. (B) Locus 14 -
410 rs72689147 (GUCY1A3) exhibits AEI in 114/121 samples across 10 different tissues.

411

412 Importantly, even one sample without AEI suggests the variant might itself not be
413 functional but rather in high LD with a functional variant and serving as a marker. With only a
414 few samples not exhibiting AEI, rs7528419 can be considered an excellent marker in tight LD
415 with the functional SNP. Furthermore, that this pattern is only found in liver suggests that the
416 regulatory variant is tissue specific. In contrast, the bidirectional ratios observed in adipose
417 tissue suggests that either the marker SNP is in low LD with a functional variant, or low
418 expression is leading to ratio deviations from unity in a random fashion. The counts in adipose
419 are relatively low (median total count 11), however it is not substantially different from liver with
420 a median count of 13.

421 The Locus 14 SNP rs72689147 (*GUCY1A3*), which falls within an intron of *GUCY1A3*,
422 exhibits AEI in 114/121 samples across 10 different tissues. Again, this SNP does not appear to

423 be functional as not all samples display AEI, but it is a robust marker. While located in an intron,
424 expression is sufficient to extract allelic ratios; as these are consistently below unity, this results
425 suggests a gain of function.

426

427 **Resolving number of signals in a locus using LD**

428 Focusing on the 7 loci where eQTL-based reprioritization pointed to a single gene as
429 well as the two examples of AEI discussed above, we find dozens of other significant eQTLs for
430 each gene. To determine whether these eQTLs represent one or more functional variants, we
431 plot the effect size (beta) of the variant on RNA expression for each eQTL against its LD (R^2)
432 with the top scoring (most significant p-value) eQTL in each tissue where eQTLs are detectable.
433 Assuming one functional variant in the locus, the beta for each eQTL should correlate with its R^2
434 relative to the highest scoring SNP (33).

435 This approach reveals that the observed eQTLs for a gene often represent more than
436 one regulatory variant, with the exception of FLT1 in Tibial Nerve – represented by only one
437 cluster of variants marked by the GWAS SNP (Fig 3). This result is critical to the correct
438 interpretation of GWAS that would otherwise rely on a single variant rather than considering the
439 combined effect of more than one causative variant.

440

441 **Fig 3. Number of eQTL signals.** Correlation plots show absolute value of beta for
442 variant effects on RNA expression versus R^2 with the top eQTL (most significant p-value),
443 including all significant eQTLs in the given gene-tissue combination. Blue dots represent the top
444 eQTL (most significant p-value), red dots represent GWAS variant(s). (A) FLT1 in Tibial Nerve:
445 eQTLs are accounted for by a single eQTL marked by the GWAS variant (all eQTLs display a
446 linear correlation with R^2). CELSR2 (liver), GUCY1A3 (tibial artery), and LIPA (blood),
447 correlation between beta and R^2 suggests multiple functional variants. (B) At least three distinct

448 LD blocks represented by LIPA eQTLs in whole blood. Correlations are shown left to right
 449 between the absolute value of beta and R^2 with rs142444 (GWAS SNP), rs1051338, or
 450 rs2250781. Tightly linked SNPs ($D' > 0.9$; $R^2 > 0.9$) are shown in the same color.

451
 452 As an example, we consider the number of distinct eQTLs needed to maximally account
 453 for LIPA expression in blood. The most significant eQTL consists of a group of SNPs in high LD
 454 marked by the GWAS variant (red dot in Fig 3), while two additional clusters of SNPs (marked
 455 by rs1051338 and rs2250781) have equally or even more robust beta and p-values but show
 456 relatively poor linkage with the GWAS cluster ($R^2 \sim 0.5$) (Fig 3B). These SNPs are more
 457 significant eQTLs than predicted by their LD with the trait-associated variant and may mark
 458 additional functional variants in the locus. To test the significance of any additional regulatory
 459 variants, we used a separate dataset (CATHGEN) to evaluate whether including an additional
 460 marker variant in a regression model improves the ability to account for LIPA expression in
 461 blood. Including additional markers improved the eQTL model, while adding a marker in strong
 462 LD with the original variant did not (Table 2), indicating there are likely multiple functional
 463 variants, incompletely represented by the GWAS variant alone, that contribute to LIPA
 464 expression in blood.

465

466 **Table 2. Assessing multiple regulatory variants for LIPA**

Variable of interest	ANOVA p-value	Model 1	Model 2
rs1412444	8.8e-16	XP ~ sex + age	XP ~ rs1412444 + sex + age
rs13332328	8.8e-16	XP ~ sex + age	XP ~ rs13332328 + sex + age
rs1051338	8.8e-16	XP ~ sex + age	XP ~ rs1051338 + sex + age
rs2250781	8.8e-16	XP ~ sex + age	XP ~ rs2250781 + sex + age
rs1412444 in context of rs13332328	1.0	XP ~ rs1412444 + sex + age	XP ~ rs1412444 + rs13332328 + sex + age

<i>rs1412444 in context of rs1051338</i>	0.23	XP ~ rs1412444 + sex + age	XP ~ rs1412444 + rs1051338 + sex + age
<i>rs1412444 in context of rs2250781</i>	0.04	XP ~ rs1412444 + sex + age	XP ~ rs1412444 + rs2250781 + sex + age
<i>rs1412444 & rs2250781 in context of rs1051338</i>	0.19	XP ~ rs1412444 + rs2250781 + sex + age	XP ~ rs1412444 + rs2250781 + rs1051338 + sex + age
<i>rs1412444 & rs1051338 in context of rs2250781</i>	0.04	XP ~ rs1412444 + rs1051338 + sex + age	XP ~ rs1412444 + rs1051338 + rs2250781 + sex + age
<i>rs1412444</i>	1e-3	MI ~ covariates	MI ~ rs1412444 + covariates
<i>rs13332328</i>	1e-3	MI ~ covariates	MI ~ rs13332328 + covariates
<i>rs1051338</i>	6e-4	MI ~ covariates	MI ~ rs1051338 + covariates
<i>rs2250781</i>	4e-4	MI ~ covariates	MI ~ rs2250781 + covariates
<i>rs1412444 in context of rs13332328</i>	0.79	MI ~ rs1412444 + covariates	MI ~ rs1412444 + rs13332328 + covariates
<i>rs1412444 in context of rs1051338</i>	0.36	MI ~ rs1412444 + covariates	MI ~ rs1412444 + rs1051338 + covariates
<i>rs1412444 in context of rs2250781</i>	0.56	MI ~ rs1412444 + covariates	MI ~ rs1412444 + rs2250781 + covariates
<i>rs1412444 & rs2250781 in context of rs1051338</i>	0.11	MI ~ rs1412444 + rs2250781 + covariates	MI ~ rs1412444 + rs2250781 + rs1051338 + covariates
<i>rs1412444 & rs1051338 in context of rs2250781</i>	0.17	MI ~ rs1412444 + rs1051338 + covariates	MI ~ rs1412444 + rs1051338 + rs2250781 + covariates

467

468 ANOVA comparing ability of models with different SNP combinations to account for LIPA
 469 expression and MI. Covariates in CATHGEN include sex, age, hypercholesterolemia, smoking,
 470 and number of diseased vessels.
 471

472 Testing these additional variants with MI instead of LIPA expression did not yield
 473 significant associations (Table 2). However, LIPA expression itself is not associated with MI
 474 except when rs1412444 is homozygous minor, which may explain the discrepancy. In looking
 475 separately at the associations between the GWAS hit and LIPA expression and the GWAS hit
 476 and MI, we find that rs1412444 is associated with increased risk of MI and increased expression
 477 of LIPA, but counterintuitively those with two minor alleles and MI exhibit lower rather than

478 higher expression, a pattern that also holds in GTEx although it is only statistically significant in
479 CATHGEN (Fig 4, S4 Figure).

480

481 **Fig 4. LIPA expression, MI, and genotype.** Comparison of LIPA expression in
482 CATHGEN for those with and without MI based on rs142444 genotype. LIPA exhibits higher
483 expression only in those without MI in the homozygous minor group (p-value = 0.02).

484

485 **Context – Tissue & Transcript specific eQTLs**

486 Genetic variation exists and functions within a context – the surrounding sequence, the
487 tissue type and its preferred transcription factors, etc. In an effort to resolve the functional
488 variation behind statistical associations observed in GWAS, it is essential to consider these
489 contexts. As highlighted by the tissue specific AEI patterns above, if these relationships are not
490 considered in a context specific manner (*e.g.*, on a tissue by tissue basis), many robust effects
491 will remain hidden. In an effort to evaluate some of these contextual features, we consider
492 tissue and transcript specific eQTLs.

493 eQTL analysis may focus the search on a relevant tissue. However, eQTLs are
494 detectable only where expression and sample size are sufficiently high; accordingly tissue-
495 specific differences in eQTLs reflect overall patterns of tissue selective expression and sample
496 size, in addition to the influence of genetic variation.

497 To consider how eQTLs for a given gene compare across different tissues, we cluster
498 genome-wide significant eQTLs reported by GTEx for LIPA in a heatmap organized by their
499 pairwise LD (R^2), using a colored bar at the top of the heatmap to denote tissue type (Fig. 5A).
500 eQTL SNPs generally cluster by tissue, suggesting distinct regulatory variants in different
501 tissues. However, there are two LD blocks that contain eQTLs in more than half of tissues
502 indicative of genetic variation that acts across different tissue types. Variants detected by

503 GWAS for LIPA appear as a significant eQTLs in a subset of tissues (Table 1), some of which fit
504 with our understanding of CAD pathology (heart, aorta, adipose), others suggest as yet
505 unexplained biological consequences (spleen, pancreas).

506

507 **Fig 5. Tissue and transcript specific eQTLs for LIPA.** (A) Heatmap of LD for those
508 SNPs reported by GTEx as genome-wide significant eQTLs for LIPA. Lighter-colored squares in
509 the heatmap represent LD blocks, with SNPs clustered by R^2 and not by genomic position.
510 Colored bars at top eQTLs in each tissue with more significant p-values denoted by darker
511 color. (B) Local Manhattan plot for *LIPA* in blood. Position is denoted on the x-axis; black bar
512 indicates gene start and stop. Negative log(p-value) for association with RNA expression is
513 denoted on the y-axis. Each transcript and the gene overall are marked by a different color (see
514 legend). Inset zooms in on the regions carrying rs1412444, rs1051338, rs2250781 identified as
515 distinct top scoring eQTLs each contributing to *LIPA* gene expression (see Fig 3).

516

517 To consider transcript-specific eQTLs more specifically, for 1mb upstream and
518 downstream of LIPA, we calculated the association between each SNP and expression of both
519 overall mRNA and individual isoforms. The resulting local Manhattan plot displays the
520 association p-values for LIPA transcripts in blood (Fig 4B). Five transcripts with no expression
521 (zero-values) in 90% or more of individuals were excluded (ENST00000428800,
522 ENST00000282673, ENST00000487618, ENST00000463623, ENST00000489359). Whereas
523 the overall eQTL patterns are similar between the gene and individual transcripts, divergent
524 SNPs indicate the presence of transcript-specific eQTLs. Remarkably, robust eQTLs distribute
525 over the entire 2 MB region, with the most distant eQTLs associated with individual transcripts
526 rather than overall gene expression. The most significant eQTLs form a peak of multiple SNPs
527 close to the transcribed region, topped by an eQTL for the gene level summary of expression

528 (ENSG00000107798) rather than any specific isoform. Tissue selectivity and functionality of
529 each transcript requires separate studies.

530

531 **Conclusions**

532 We consider each of 58 loci implicated in CAD by GWAS to better understand the
533 biological meaning of the underlying statistical associations. In evaluating each of these loci, we
534 find numerous candidate genes that were not included in the original annotation by GWAS.
535 Many of these are non-coding. Non-coding RNAs, now well-recognized for their role as
536 regulators, have historically been dismissed and continue to be difficult to study, a trend that is
537 apparent in their poor representation in the literature, among GO annotations, and as annotated
538 by GWAS (26). We find no evidence to suggest these non-coding RNAs are less likely to
539 account for the observed associations in GWAS and would advocate for their inclusion in further
540 mechanistic and computational work examining these loci. In addition to broadening candidate
541 gene lists to include non-coding transcripts, we would urge reconsideration of current
542 assignments, especially for those loci categorized as Tier2C where expression, splicing, and
543 physical position do not support the gene annotated by GWAS. LDLR is a particularly prominent
544 example. Given our understanding of the critical role lipid metabolism plays in CAD, it is
545 counterintuitive not to assign a CAD GWAS variant to LDLR when it lies within 15kb of the
546 *LDLR* locus (34). However, RNA expression and splicing data do not support this annotation,
547 instead supporting the notion that such genetic variation affects the function of other nearby
548 genes including SMARCA4, CARM1, YIPF2, RGL3, SLC44A2 (29).

549 Using allelic ratios built from tissue-specific RNA sequencing data available through GTEx,
550 we were able to identify two loci where the GWAS variant served as a robust marker for a
551 functional *cis*-acting regulatory variant. Locus 3 – rs7528419 (SORT1) falls in the 3'UTR of
552 CELSR2, exhibits AEI exclusively in liver, and is in nearly perfect LD with rs12740374 which

553 was shown by Musunuru et al. through a series of molecular experiments to create a C/EBP
554 binding site increasing expression of SORT1, a multiligand sorting receptor which they
555 concomitantly showed to be associated with LDL-C and VLDL levels (35). This work revealed a
556 single functional variant for a single target gene with a substantial effect size, the authors
557 estimated a ~40% difference in MI risk. Our work suggests additional eQTLs not explained by
558 their LD with the LD block marked by GWAS variant rs7528419. As we begin to identify
559 functional variation behind GWAS associations, an important next step will be resolving
560 additional functional variants within the loci that may modify these associations and better
561 account for disease risk (36).

562 This work emphasizes that the linear presentation of GWAS results as a single variant tied
563 to a single gene fails to capture the complexity of these loci. Many loci contain several SNPs
564 identified by GWAS, and for each of these, multiple candidate genes are implicated by RNA
565 expression and splicing associations as well as physical proximity. LD alone rarely accounts for
566 the observed eQTLs, suggesting multiple functional variants within these loci. Extending the
567 search for functional variants implicated by GWAS over a larger genomic region (1 Mb) can
568 further reveal novel candidate loci. Although some GWAS associations may ultimately implicate
569 single variants that alter expression of individual genes, this work indicates that true genetic
570 effect size of a gene locus is accounted for by a multi-factorial system that allows for multiple
571 functional variants regulating one or more genes. The approach presented here must be
572 expanded to include functional variants that are undetectable by RNAseq of whole tissues,
573 including cell type specific expression, effect on RNA-protein interactions, distribution in sub-
574 cellular domains, alteration of translational processes, and of course variants that change
575 protein functions.

576

577 **Acknowledgements**

578 This study was supported by National Institutes of Health National Institute of General
579 Medical Science Pharmacogenetics Research Network [Grant U01 GM092655] and the
580 National Center for Advancing Translational Sciences [TL1 TR001069].

581 The GTEx Project was supported by the Common Fund of the Office of the Director of
582 the National Institutes of Health, and by NCI, NHGRI, NHLBI, NIDA, NIMH, and NINDS. The
583 data used for the analyses described in this manuscript were obtained from: the GTEx Portal
584 and dbGaP accession number phs000424.

585 For CATHGEN, clinical data originated from the Duke Databank for Cardiovascular
586 Disease (DDCD) and biological samples originated from the Duke Cardiac CATHeterization
587 (CATHGEN) study. Funding support for the Genetic Mediators of Metabolic CVD Risk was
588 provided by NHLBI grant RC2 HL101621 (William E. Kraus). The data used for the analyses
589 described in this manuscript were obtained from the dbGaP accession number
590 phs0000703.v1.p1.

591 Computing time provided by the Ohio Supercomputer Center, GRANT #: PAS0885-2
592 and the Prometheus Cyfronet AGH.

593

594 **References**

- 595 1. Nikpay M, Goel A, Won H-H, Hall LM, Willenborg C, Kanoni S, et al. A comprehensive
596 1000 Genomes–based genome-wide association meta-analysis of coronary artery
597 disease. *Nat Genet* [Internet]. 2015 Sep 7 [cited 2016 Jun 28];47(10):1121–30. Available
598 from: <http://www.nature.com/doi/10.1038/ng.3396>
- 599 2. Inouye M, Abraham G, Nelson CP, Wood AM, Sweeting MJ, Dudbridge F, et al. Genomic
600 Risk Prediction of Coronary Artery Disease in 480,000 Adults: Implications for Primary
601 Prevention. *J Am Coll Cardiol* [Internet]. 2018 Oct 16 [cited 2020 Oct 22];72(16):1883–93.
602 Available from: <https://doi.org/10.1016/j.jacc.2018.07.079>

- 603 3. Musunuru K, Kathiresan S. Genetics of Common, Complex Coronary Artery Disease. Vol.
604 177, Cell. Cell Press; 2019. p. 132–45.
- 605 4. Nurnberg ST, Zhang H, Hand NJ, Bauer RC, Saleheen D, Reilly MP, et al. From Loci to
606 Biology. *Circ Res* [Internet]. 2016 Feb 19 [cited 2017 Jul 1];118(4):586–606. Available
607 from: <http://www.ncbi.nlm.nih.gov/pubmed/26892960>
- 608 5. Hindorff LA, Sethupathy P, Junkins HA, Ramos EM, Mehta JP, Collins FS, et al. Potential
609 etiologic and functional implications of genome-wide association loci for human diseases
610 and traits. *Proc Natl Acad Sci U S A*. 2009;106:9362–7.
- 611 6. Smemo S, Tena JJ, Kim K-H, Gamazon ER, Sakabe NJ, Gómez-Marín C, et al. Obesity-
612 associated variants within FTO form long-range functional connections with IRX3. *Nature*
613 [Internet]. 2014 Mar 20 [cited 2015 Jun 29];507(7492):371–5. Available from:
614 <http://dx.doi.org/10.1038/nature13138>
- 615 7. Won HH, Natarajan P, Dobbyn A, Jordan DM, Roussos P, Lage K, et al. Disproportionate
616 Contributions of Select Genomic Compartments and Cell Types to Genetic Risk for
617 Coronary Artery Disease. Snyder M, editor. *PLoS Genet* [Internet]. 2015 Oct 28 [cited
618 2016 Jun 28];11(10):e1005622. Available from:
619 <http://dx.plos.org/10.1371/journal.pgen.1005622>
- 620 8. Johnson AD, Zhang Y, Papp AC, Pinsonneault JK, Lim J-E, Saffen D, et al.
621 Polymorphisms affecting gene transcription and mRNA processing in pharmacogenetic
622 candidate genes: detection through allelic expression imbalance in human target tissues.
623 *Pharmacogenet Genomics* [Internet]. 2008 Sep [cited 2016 Jul 15];18(9):781–91.
624 Available from: <http://www.ncbi.nlm.nih.gov/pubmed/18698231>
- 625 9. Barrie ES, Hartmann K, Lee S-H, Frater JT, Seweryn M, Wang D, et al. The
626 CHRNA5/CHRNA3/CHRNA4 Nicotinic Receptor Regulome: Genomic Architecture,
627 Regulatory Variants, and Clinical Associations. *Hum Mutat* [Internet]. 2016 Nov [cited
628 2016 Dec 9]; Available from: <http://doi.wiley.com/10.1002/humu.23135>

- 629 10. Halley P, Kadakkuzha BM, Faghihi MA, Magistri M, Zeier Z, Khorkova O, et al.
630 Regulation of the apolipoprotein gene cluster by a long noncoding RNA. *Cell Rep*
631 [Internet]. 2014 Jan 16 [cited 2015 Jan 16];6(1):222–30. Available from:
632 [http://www.pubmedcentral.nih.gov/articlerender.fcgi?artid=3924898&tool=pmcentrez&ren](http://www.pubmedcentral.nih.gov/articlerender.fcgi?artid=3924898&tool=pmcentrez&rendertype=abstract)
633 [dertype=abstract](http://www.pubmedcentral.nih.gov/articlerender.fcgi?artid=3924898&tool=pmcentrez&rendertype=abstract)
- 634 11. Tada H, Won HH, Melander O, Yang J, Peloso GM, Kathiresan S. Multiple associated
635 variants increase the heritability explained for plasma lipids and coronary artery disease.
636 *Circ Cardiovasc Genet* [Internet]. 2014 Oct 1 [cited 2016 Jun 28];7(5):583–7. Available
637 from: <http://circgenetics.ahajournals.org/cgi/doi/10.1161/CIRCGENETICS.113.000420>
- 638 12. Wang D, Hartmann K, Seweryn M, Sadee W. Interactions Between Regulatory Variants
639 in CYP7A1 (Cholesterol 7 α -Hydroxylase) Promoter and Enhancer Regions Regulate
640 CYP7A1 Expression. *Circ Genomic Precis Med* [Internet]. 2018 [cited 2020 Jul
641 12];11(10):e002082. Available from: <http://www.ncbi.nlm.nih.gov/pubmed/30354296>
- 642 13. Lippert C, Listgarten J, Davidson RI, Baxter S, Poon H, Poong H, et al. An exhaustive
643 epistatic SNP association analysis on expanded Wellcome Trust data. *Sci Rep* [Internet].
644 2013 Jan [cited 2015 Jan 12];3:1099. Available from:
645 [http://www.pubmedcentral.nih.gov/articlerender.fcgi?artid=3551227&tool=pmcentrez&ren](http://www.pubmedcentral.nih.gov/articlerender.fcgi?artid=3551227&tool=pmcentrez&rendertype=abstract)
646 [dertype=abstract](http://www.pubmedcentral.nih.gov/articlerender.fcgi?artid=3551227&tool=pmcentrez&rendertype=abstract)
- 647 14. Hemani G, Knott S, Haley C, Li Z, Wang S. An Evolutionary Perspective on Epistasis and
648 the Missing Heritability. Mackay TFC, editor. *PLoS Genet* [Internet]. 2013 Feb 28 [cited
649 2017 Aug 8];9(2):e1003295. Available from:
650 <http://dx.plos.org/10.1371/journal.pgen.1003295>
- 651 15. Hartmann K, Seweryn M, Handleman SK, Rempala GA, Sadee W. Non-linear
652 interactions between candidate genes of myocardial infarction revealed in mRNA
653 expression profiles. *BMC Genomics* [Internet]. 2016 [cited 2016 Oct 12];17(1):738.
654 Available from: <http://www.ncbi.nlm.nih.gov/pubmed/27640124>

- 655 16. Skwark MJ, Croucher NJ, Puranen S, Chewapreecha C, Pesonen M, Xu YY, et al.
656 Interacting networks of resistance, virulence and core machinery genes identified by
657 genome-wide epistasis analysis. Gojobori T, editor. PLOS Genet [Internet]. 2017 Feb 16
658 [cited 2020 Oct 22];13(2):e1006508. Available from:
659 <https://dx.plos.org/10.1371/journal.pgen.1006508>
- 660 17. Nie SF, Zha LF, Fan Q, Liao YH, Zhang HS, Chen QW, et al. Genetic regulation of the
661 thymic stromal lymphopoietin (TSLP)/TSLP receptor (TSLPR) gene expression and
662 influence of epistatic interactions between IL-33 and the TSLP/TSLPR axis on risk of
663 coronary artery disease. Front Immunol [Internet]. 2018 Aug 3 [cited 2020 Oct
664 22];9(AUG):3. Available from: [/pmc/articles/PMC6085432/?report=abstract](https://pubmed.ncbi.nlm.nih.gov/30111111/)
- 665 18. Rio S, Mary-Huard T, Moreau L, Bauland C, Palaffre C, Madur D, et al. Disentangling
666 group specific QTL allele effects from genetic background epistasis using admixed
667 individuals in GWAS: An application to maize flowering. Springer NM, editor. PLOS
668 Genet [Internet]. 2020 Mar 4 [cited 2020 Oct 22];16(3):e1008241. Available from:
669 <https://dx.plos.org/10.1371/journal.pgen.1008241>
- 670 19. Wallace C, Rotival M, Cooper JD, Rice CM, Yang JHM, McNeill M, et al. Statistical
671 colocalization of monocyte gene expression and genetic risk variants for type 1 diabetes.
672 Hum Mol Genet [Internet]. 2012 Jun 15 [cited 2020 Oct 22];21(12):2815–24. Available
673 from: <http://cran.r-project.org>
- 674 20. Giambartolomei C, Vukcevic D, Schadt EE, Franke L, Hingorani AD, Wallace C, et al.
675 Bayesian Test for Colocalisation between Pairs of Genetic Association Studies Using
676 Summary Statistics. Williams SM, editor. PLoS Genet [Internet]. 2014 May 15 [cited 2020
677 Oct 22];10(5):e1004383. Available from:
678 <https://dx.plos.org/10.1371/journal.pgen.1004383>
- 679 21. Hormozdiari F, van de Bunt M, Segrè A V., Li X, Joo JWJ, Bilow M, et al. Colocalization
680 of GWAS and eQTL Signals Detects Target Genes. Am J Hum Genet. 2016 Dec

- 681 1;99(6):1245–60.
- 682 22. Lonsdale J, Thomas J, Salvatore M, Phillips R, Lo E, Shad S, et al. The Genotype-Tissue
683 Expression (GTEx) project. *Nat Genet* [Internet]. 2013 Jun [cited 2014 Jul 10];45(6):580–
684 5. Available from: <http://dx.doi.org/10.1038/ng.2653>
- 685 23. C G, J ZL, W Z, M H, H S, J B, et al. A Bayesian Framework for Multiple Trait
686 Colocalization From Summary Association Statistics. *Bioinformatics* [Internet]. 2018 [cited
687 2020 Jun 12];34(15). Available from:
688 https://pubmed.ncbi.nlm.nih.gov/29579179/?from_term=COLOC&from_pos=2
- 689 24. F W, CQ X, Q H, JP C, XC L, D W, et al. Genome-wide Association Identifies a
690 Susceptibility Locus for Coronary Artery Disease in the Chinese Han Population. *Nat*
691 *Genet* [Internet]. 2011 [cited 2020 Jun 12];43(4). Available from:
692 <https://pubmed.ncbi.nlm.nih.gov/21378986/>
- 693 25. Wainberg M, Sinnott-Armstrong N, Mancuso N, Barbeira AN, Knowles DA, Golan D, et al.
694 Opportunities and challenges for transcriptome-wide association studies. *Nat Genet*.
695 2019;51(4).
- 696 26. Mongelli A, Martelli F, Farsetti A, Gaetano C. The dark that matters: Long noncoding
697 RNAs as master regulators of cellular metabolism in noncommunicable diseases
698 [Internet]. Vol. 10, *Frontiers in Physiology*. Frontiers Media S.A.; 2019 [cited 2020 Oct
699 22]. p. 369. Available from: www.frontiersin.org
- 700 27. Lee DP, Tan WLW, Anene-Nzelu CG, Lee CJM, Li PY, Luu TDA, et al. Robust CTCF-
701 Based Chromatin Architecture Underpins Epigenetic Changes in the Heart Failure
702 Stress–Gene Response. *Circulation* [Internet]. 2019 Apr 16 [cited 2020 Oct
703 22];139(16):1937–56. Available from:
704 <https://www.ahajournals.org/doi/10.1161/CIRCULATIONAHA.118.036726>
- 705 28. Sadee W, Hartmann K, Seweryn M, Pietrzak M, Handelman SK, Rempala GA. Missing
706 heritability of common diseases and treatments outside the protein-coding exome. *Hum*

- 707 Genet [Internet]. 2014 Oct [cited 2015 Jan 16];133(10):1199–215. Available from:
708 <http://www.ncbi.nlm.nih.gov/pubmed/25107510>
- 709 29. Mascarenhas R, Pietrzak M, Smith RM, Webb A, Wang D, Papp AC, et al. Allele-
710 Selective Transcriptome Recruitment to Polysomes Primed for Translation: Protein-
711 Coding and Noncoding RNAs, and RNA Isoforms. PLoS One [Internet]. 2015 Jan 2 [cited
712 2016 Feb 6];10(9):e0136798. Available from:
713 <http://journals.plos.org/plosone/article?id=10.1371/journal.pone.0136798>
- 714 30. Jones PD, Webb TR. From GWAS to new biology and treatments in CAD. Aging (Albany
715 NY) [Internet]. 2019 [cited 2020 Jun 12];11(6):1611. Available from:
716 <https://www.ncbi.nlm.nih.gov/pmc/articles/PMC6461175/>
- 717 31. Lu R, Smith RM, Seweryn M, Wang D, Hartmann K, Webb A, et al. Analyzing allele
718 specific RNA expression using mixture models. BMC Genomics [Internet]. 2015 Jan 1
719 [cited 2016 Jan 29];16(1):566. Available from:
720 <http://bmcbgenomics.biomedcentral.com/articles/10.1186/s12864-015-1749-0>
- 721 32. Smith RM, Webb A, Papp AC, Newman LC, Handelman SK, Suhy A, et al. Whole
722 transcriptome RNA-Seq allelic expression in human brain. BMC Genomics [Internet].
723 2013 Jan [cited 2015 Jan 2];14:571. Available from:
724 [http://www.pubmedcentral.nih.gov/articlerender.fcgi?artid=3765493&tool=pmcentrez&ren
725 dertype=abstract](http://www.pubmedcentral.nih.gov/articlerender.fcgi?artid=3765493&tool=pmcentrez&rendertype=abstract)
- 726 33. Ni G, Moser G, Ripke S, Neale BM, Corvin A, Walters JTR, et al. Estimation of Genetic
727 Correlation via Linkage Disequilibrium Score Regression and Genomic Restricted
728 Maximum Likelihood. Am J Hum Genet. 2018;102(6).
- 729 34. Roberts R. Genetics of coronary artery disease: an update. Methodist Debaquey
730 Cardiovasc J [Internet]. 2014 Jan [cited 2015 Jul 28];10(1):7–12. Available from:
731 [http://www.pubmedcentral.nih.gov/articlerender.fcgi?artid=4051327&tool=pmcentrez&ren
732 dertype=abstract](http://www.pubmedcentral.nih.gov/articlerender.fcgi?artid=4051327&tool=pmcentrez&rendertype=abstract)

- 733 35. Musunuru K, Strong A, Frank-Kamenetsky M, Lee NE, Ahfeldt T, Sachs K V., et al. From
734 noncoding variant to phenotype via SORT1 at the 1p13 cholesterol locus. Nature
735 [Internet]. 2010 Aug 5 [cited 2020 Oct 22];466(7307):714–9. Available from:
736 <https://pubmed.ncbi.nlm.nih.gov/20686566/>
- 737 36. Crouch DJM, Bodmer WF. Polygenic inheritance, GWAS, polygenic risk scores, and the
738 search for functional variants. 2020;117(32):18924–33.

739

740 **Supporting information**

741 **S1 File. Fig 1 Gene Names.** Gene names corresponding to bar plot presented in Fig 1

742 B.

743 **S2 File. Example locus.** Example of a locus (*LIPA*) implicated by GWAS taken from
744 ensemble.org. There are numerous annotated protein-coding and non-coding transcripts in
745 close proximity and overlapping one another.

746 **S3 File. 58 CAD GWAS loci.** Table of 58 GWAS loci including tier designation, SNPs
747 considered, GWAS annotation, and genes introduced by eQTL, sQTL, and position.

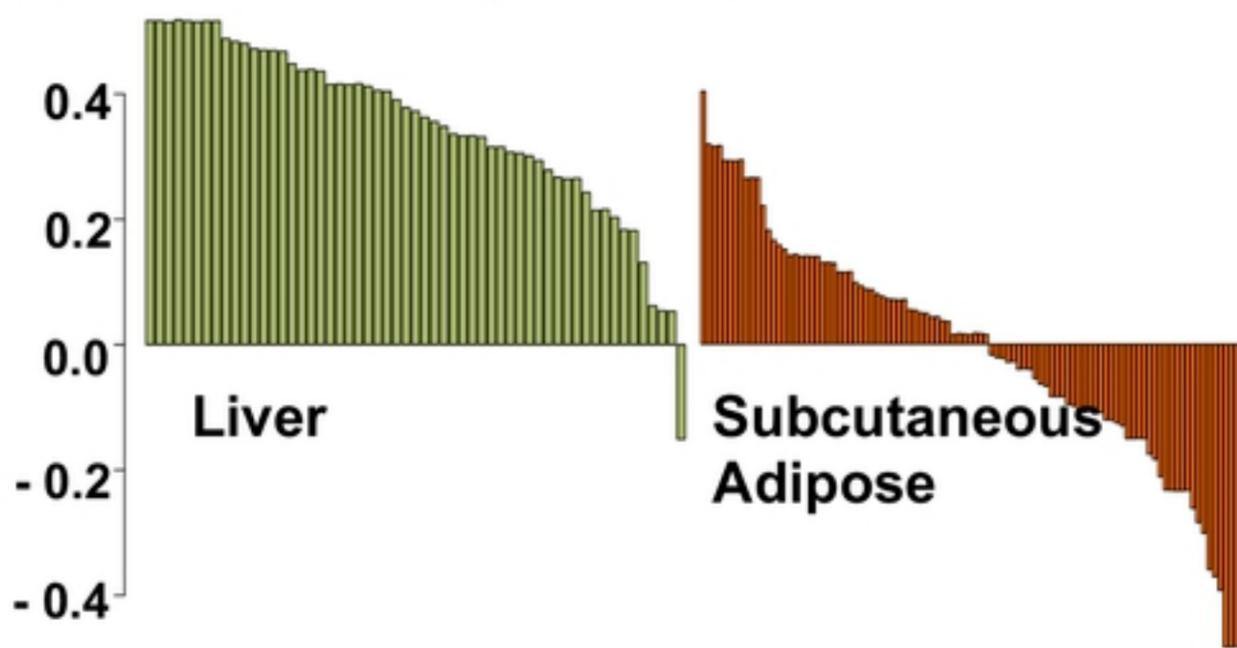
748 **S1 Fig. Expanding candidate genes process.** Flowchart portraying process of
749 expanding candidate gene list from 75 to 245 using eQTL, sQTL, and physical position.

750 **S2 Fig. Tier assignment process.** Flowchart portraying process of assigning tiers to
751 CAD GWAS loci.

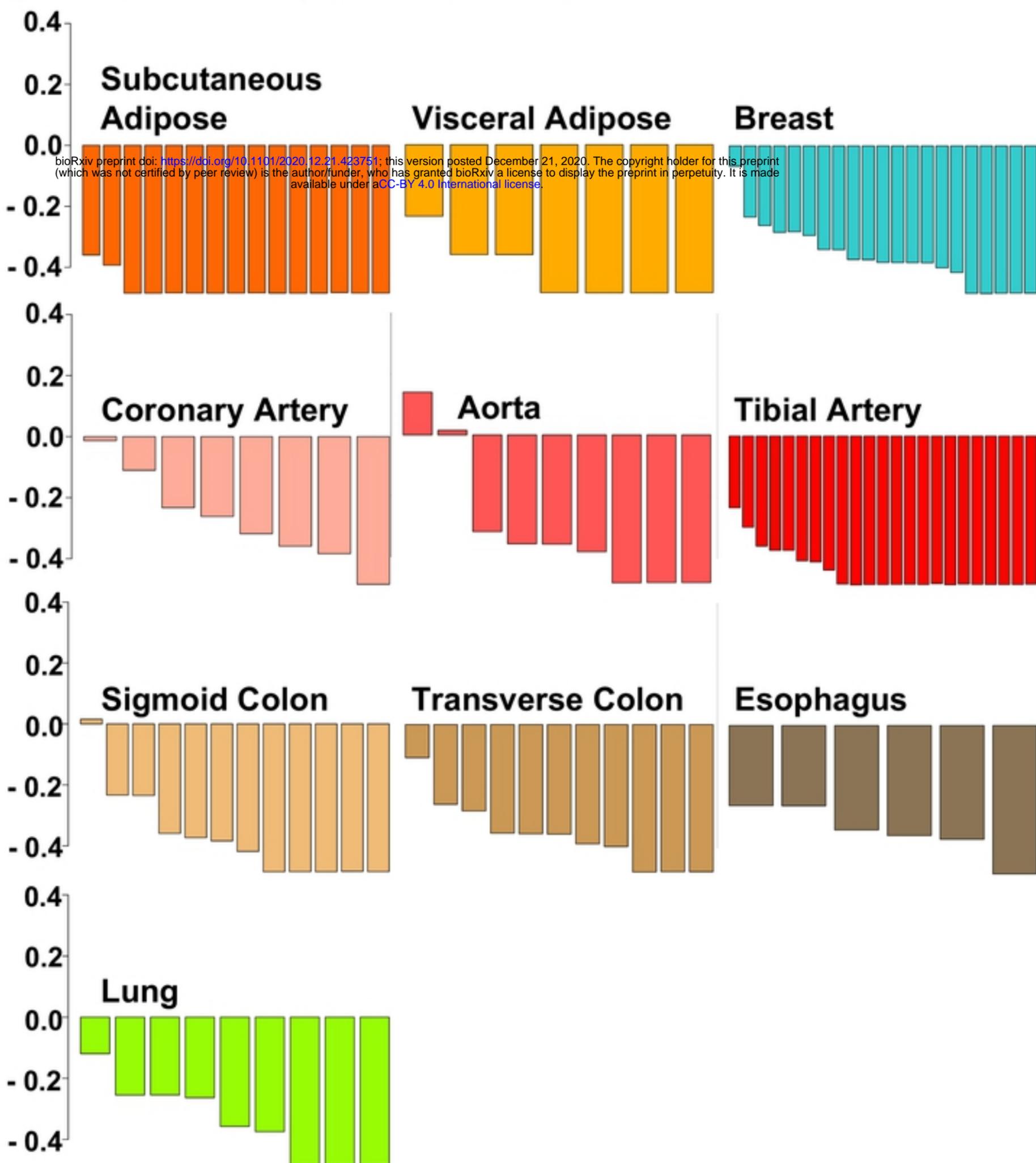
752 **S3 Fig. eQTL, sQTL, position Venn diagram.** Venn diagram showing overlap in
753 candidate genes derived from eQTL, sQTL, and position-based re-prioritization.

754 **S4 Fig. LIPA expression, CAD, and genotype in GTEx.** Comparison of LIPA
755 expression in GTEx for those with and without heart disease based on rs142444 genotype.
756 LIPA exhibits higher expression in those without heart disease only in the homozygous minor
757 group (p value = 0.22).

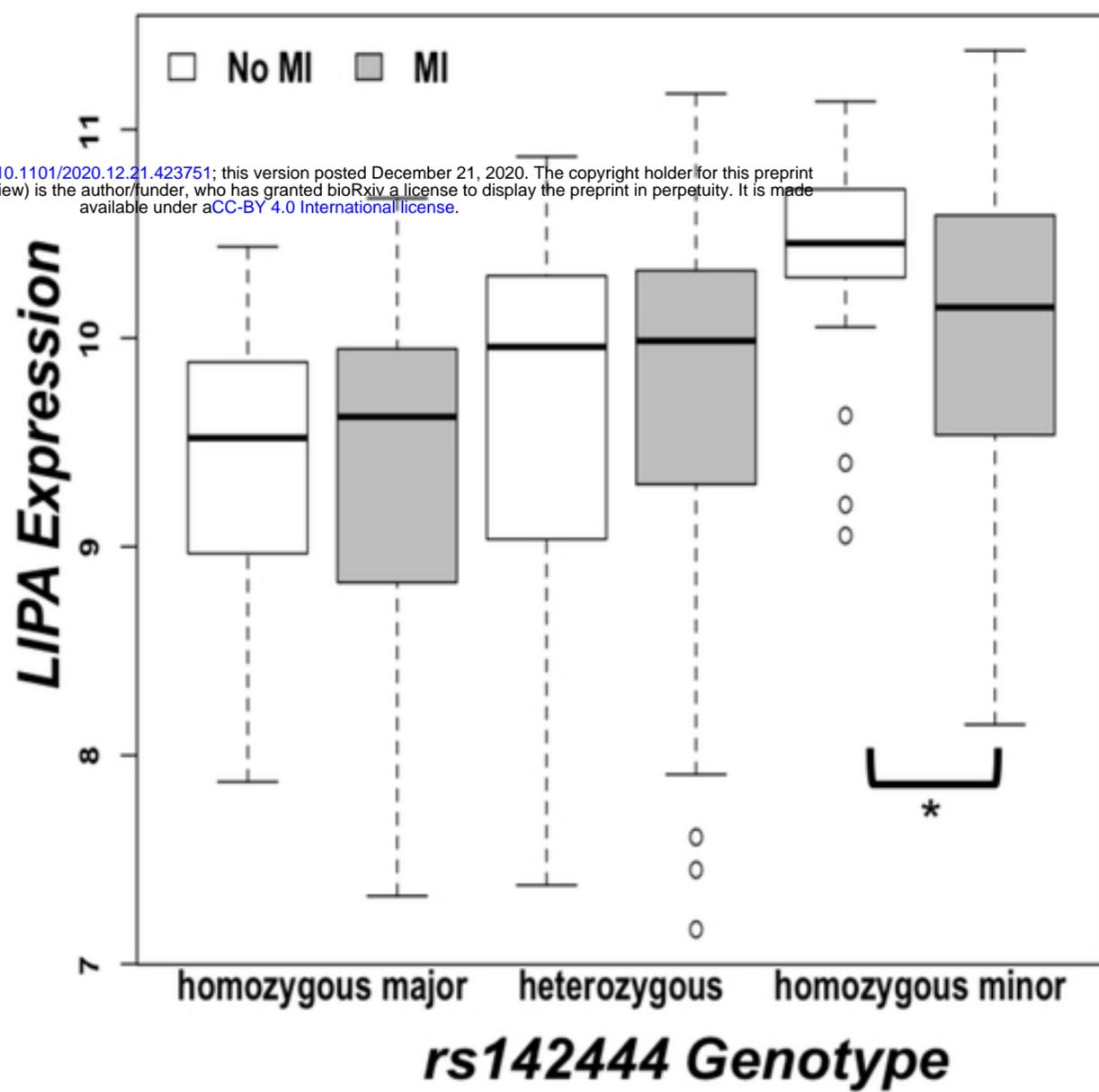
A rs7528419, SORT1 LOCUS



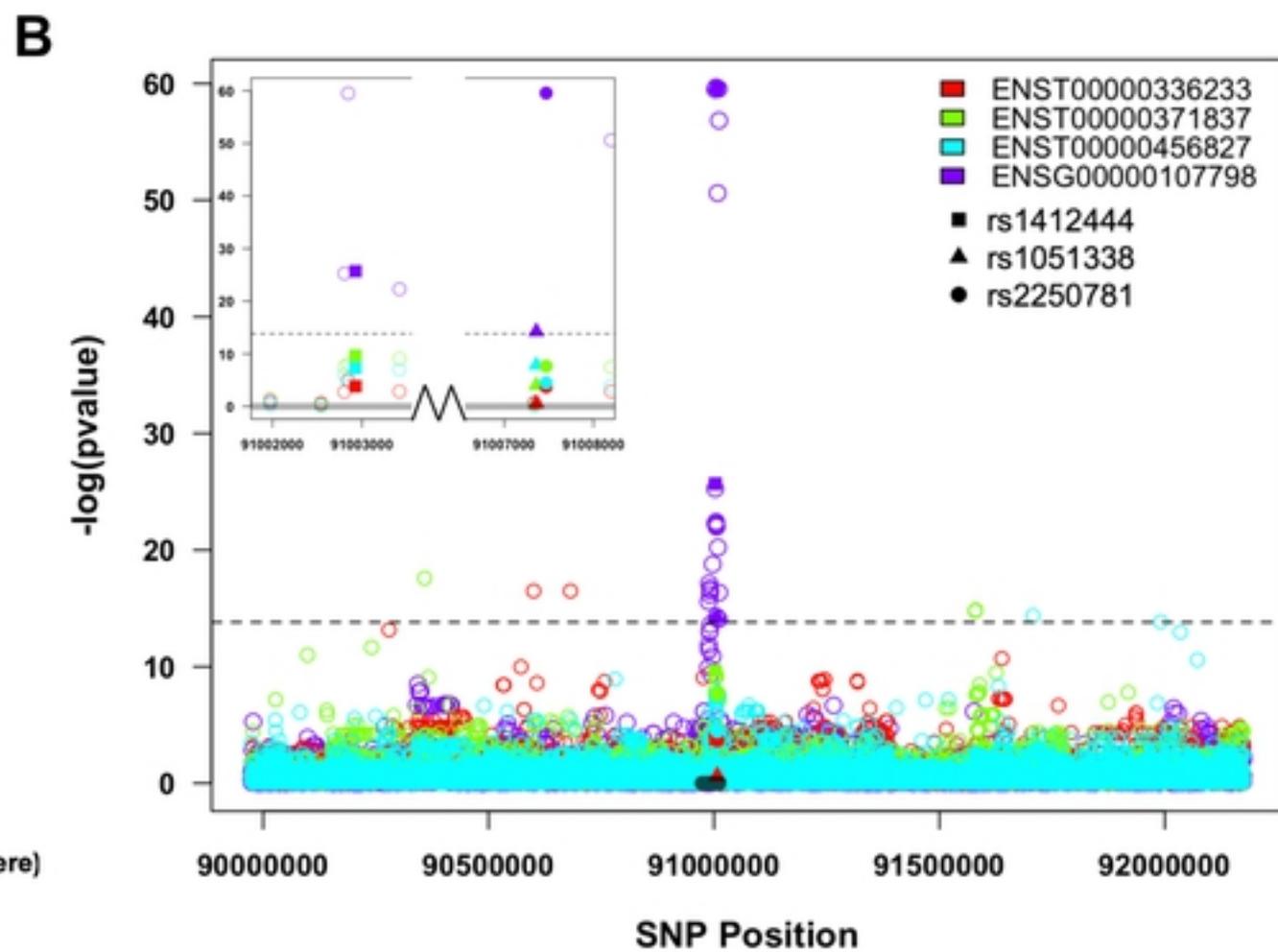
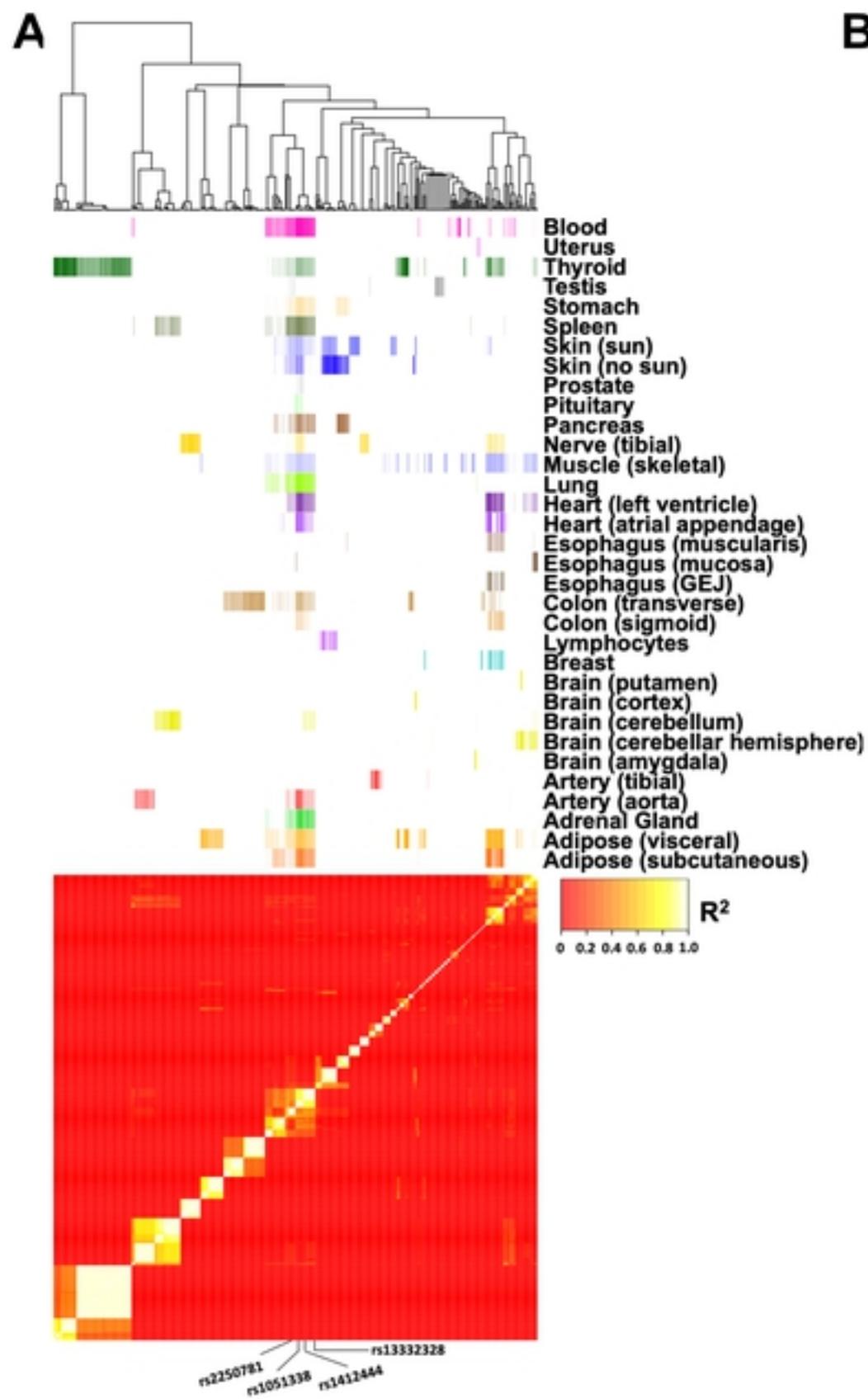
B rs72689147, GUCY1A3 LOCUS



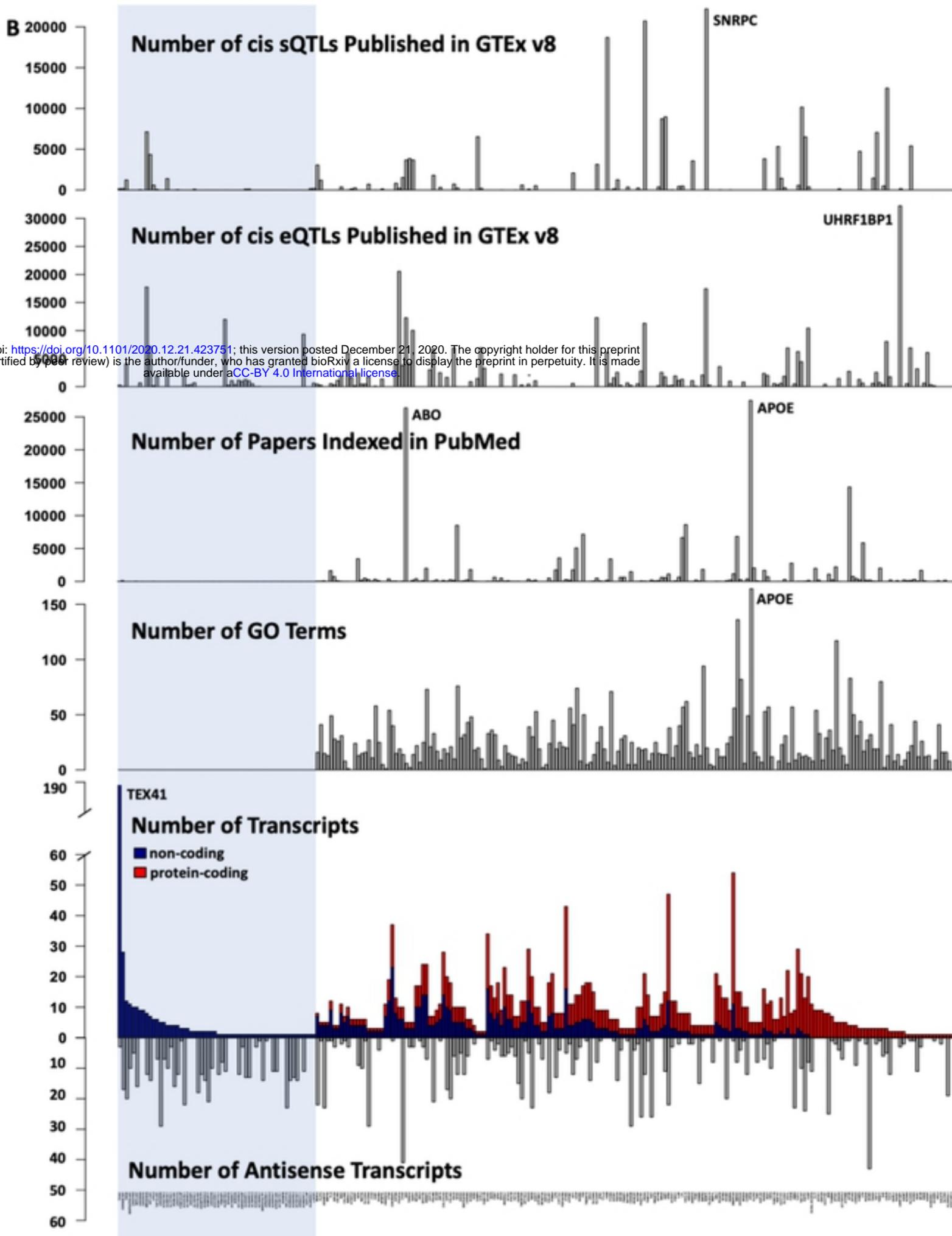
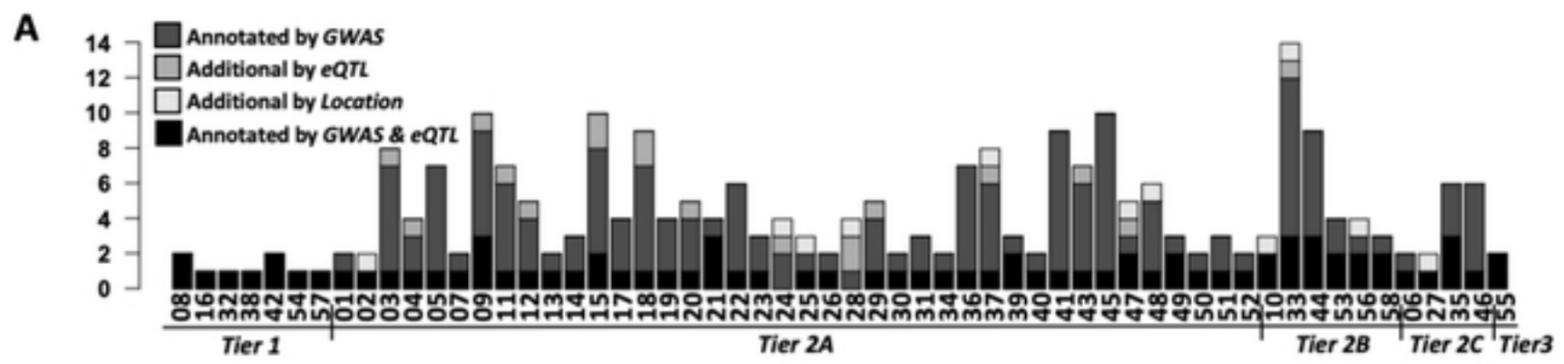
bioRxiv preprint doi: <https://doi.org/10.1101/2020.12.21.423751>; this version posted December 21, 2020. The copyright holder for this preprint (which was not certified by peer review) is the author/funder, who has granted bioRxiv a license to display the preprint in perpetuity. It is made available under aCC-BY 4.0 International license.



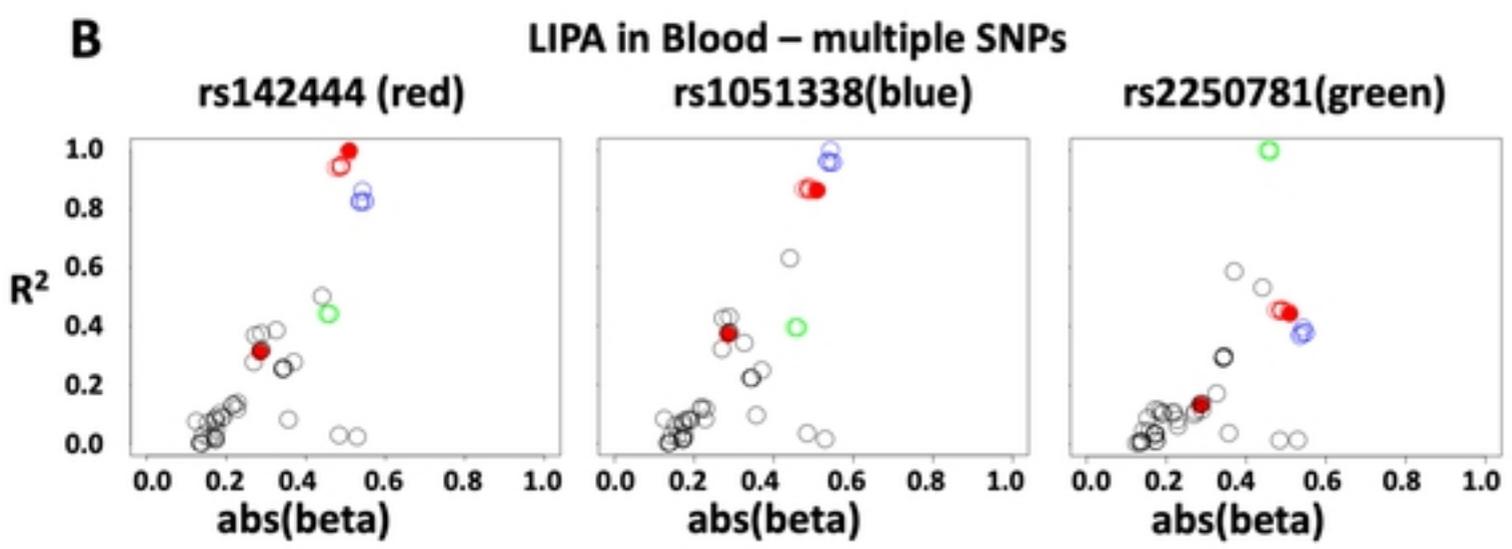
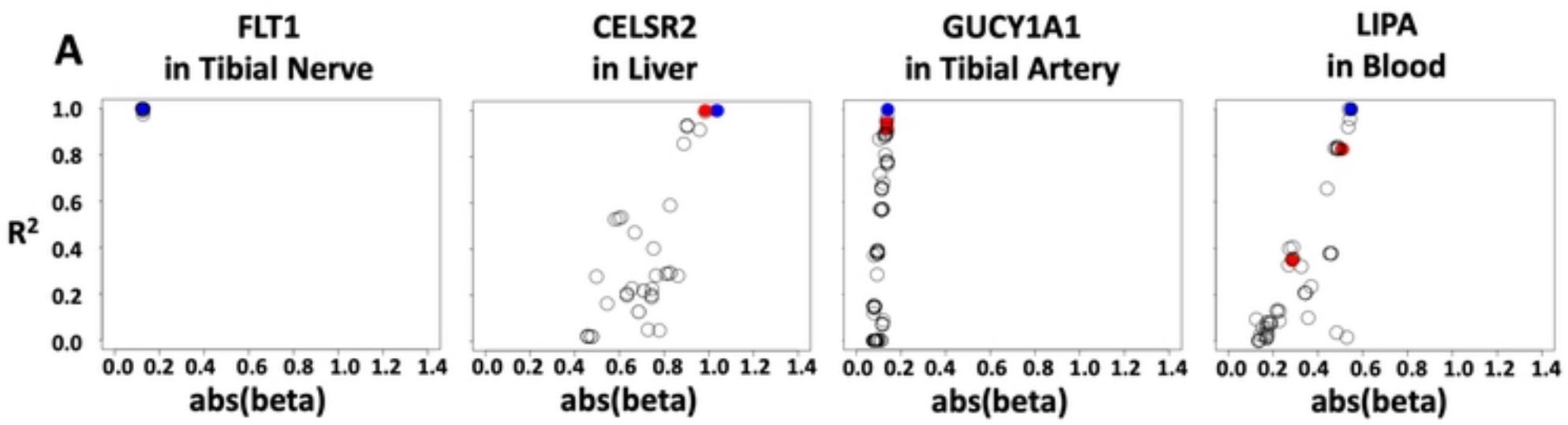
Figure



Figure



bioRxiv preprint doi: <https://doi.org/10.1101/2020.12.21.423751>; this version posted December 21, 2020. The copyright holder for this preprint (which was not certified by peer review) is the author/funder, who has granted bioRxiv a license to display the preprint in perpetuity. It is made available under aCC-BY 4.0 International license.



Figure